Submicrosecond Phospholipid Dynamics Using a Long-Lived Fluorescence Emission Anisotropy Probe

Lesley Davenport and Piotr Targowski
Department of Chemistry, Brooklyn College of the City University of New York, Brooklyn, New York 11210 USA

ABSTRACT The use of the long-lived fluorescence probe coronene ($\langle\tau_{FL}\rangle \approx 200$ ns) is described for investigating submicrosecond lipid dynamics in DPPC model bilayer systems occurring below the lipid phase transition. Time-resolved fluorescence emission anisotropy decay profiles, measured as a function of increasing temperature toward the lipid-phase transition temperature (T_c), for coronene-labeled DPPC small unilamellar vesicles (SUVs), are best described in most cases by three rotational decay components ($\phi_{i=3}$). We have interpreted these data using two dynamic lipid bilayer models. In the first, a compartmental model, the long correlation time (ϕ_N) is assigned to immobilized coronene molecules located in "gel-like" or highly ordered lipid phases ($S\rightarrow1$) of the bilayer, whereas a second fast rotational time ($\phi_F \approx 2$–5 ns) is associated with probes residing in more "fluid-like" regions (with corresponding lower ordering, $S\rightarrow0$). Interests here have focused on the origins of an intermediate correlation time (50–100 ns), the associated amplitude (β_G) of which increases with increasing temperature. Such behavior suggests a changing rotational environment surrounding the coronene molecules, arising from fluidization of gel lipid. The observed effective correlation time (ϕ_{EFF}) thus reflects a discrete gel-fluid lipid exchange rate (k_{FG}). A refinement of the compartmental model invokes a distribution of gel-fluid exchange rates ($d(S,T)$) corresponding to a distribution of lipid order parameters and is based on an adapted Landau expression for describing "gated" packing fluctuations. A total of seven parameters (five thermodynamic quantities, defined by the free energy versus temperature expansion; one gating parameter (γ) defining a cooperative "melting" requirement; one limiting diffusion rate (or frequency factor: d_∞)) suffice to predict complete anisotropy decay curves measured for coronene at several temperatures below the phospholipid T_c. The thermodynamic quantities are associated with the particular lipid of interest (in this case DPPC) and have been determined previously from ultrasound studies, thus representing fixed constants. Hence resolved variables are r_0, temperature-dependent gate parameters (γ), and limiting diffusion rates (d_∞). This alternative distribution model is attractive because it provides a general and probe-independent expression for distributed lipid fluctuation-induced probe rotational rates occurring within bilayer membranes below the phospholipid phase transition on the submicrosecond time scale.

INTRODUCTION

Experimental fluorescence studies of dynamic lipid packing fluctuations or "gel-fluid" exchange occurring within bilayer membranes have been limited, although (static) microheterogeneity of lipid packing has been studied extensively (Chen et al., 1977; Kawato et al., 1977; Klausner et al., 1980; Wolber and Hudson, 1981; Chong and Weber, 1983; Davenport et al., 1986, 1989; Sieber, 1987; Mateo et al., 1991, 1993a; Parassasi et al., 1993). Current knowledge of lipid dynamics has arisen primarily from theoretical modeling of (phenomenological, e.g., long-range Landau theory; Jähnig, 1981a,b) or microscopic statistical mechanical approaches to (Doniach, 1978; Zuckermann et al., 1982; Mouritsen et al., 1983; Mouritsen and Zuckerman, 1985; Ipsen et al., 1990) events occurring at the lipid phase transition, where lipid microheterogeneity is clearly evident. Here strong lateral density fluctuations between neighboring lipid molecules result in the appearance of gel (ordered) and fluid (disordered) lipid clusters, coexisting as a dynamic gel-fluid equilibrium. The terms "gel" and "fluid" refer to a wide range of acyl-chain conformational order. Not directly visible by microscopy tools, these lipid clusters are composed of only a few tens of molecules, in contrast to larger (micrometer-sized) and more chemically heterogeneous membrane "domains" (Wolf and Voglmayr, 1984; Edidin, 1992; Thomas et al., 1994).

It is proposed that thermodynamic fluctuations of lipid order, both positional (lateral) and conformational (along the fatty-acyl chain), are responsible for many important and observable membrane-mediated events, ranging from passive transport of Na^+ ions through the bilayer at the phospholipid lipid phase transition temperature (T_c) (Nagle and Scott, 1978; Kanehisa and Tsong, 1978) to maintenance of fluidity gradients (Wardlaw et al., 1987), bilayer compressibility (Albrecht et al., 1978), and water-mediated "hydration repulsion" between interacting membranes (Goldstein and Leibler, 1989). The size distribution of such lipid clusters and their time-dependent alteration in size can thus potentially lead to specialized membrane properties.

Experimental limitations on the investigation of such important lipid dynamics have arisen because of the time scale over which the lipid fluctuations are expected to occur. Previous studies have exploited a number of biophysical approaches, ranging from macromolecular (e.g., differential scanning calorimetry; Imaizumi and Garland, 1987; Bil-

Received for publication 28 March 1996 and in final form 17 July 1996.

Address reprint requests to Dr. Lesley Davenport, Department of Chemistry, Brooklyn College of the City University of New York, 2900 Bedford Avenue, Brooklyn, NY 11210. Tel: 718-951-5750; Fax: 718-951-4827; E-mail: ladbc@cunyvm.cuny.edu.

Dr. Targowski's permanent address is Institute of Physics, Nicholas Copernicus University, ul Grudziadzka 5, 87–100 Torun, Poland.

0006-3495/96/10/1837/16 $2.00

tonen, 1990), to more localized probe studies (e.g., fluorescence: Davenport et al., 1988; Ruggiero and Hudson, 1989; Davenport and Targowski, 1995; and NMR: Hawton and Doane, 1987). From analogy with nematic crystals, relaxation times for such processes are expected to be on the order of 10^{-7} s (deGennes and Prost, 1993). Dielectric and ultrasound studies (Mitaku et al., 1978, 1983; Michels et al., 1989) of lipid membranes report relaxation times consistent with this expectation.

Further evidence for persistent lipid motions is suggested from comparison of order parameters ($S = (r_\infty/r_0)^{1/2}$), determined using a wide variety of physical methods and membrane systems. The large variability in the magnitude of the order parameters determined from magnetic resonance methods (ESR; Hubbell and McConnell, 1971; Jost et al., 1971), proton (^{1}H) (Seiter and Chan, 1973) and deuterium (^{2}H) NMR (Seelig and Seelig, 1974a; Stockton et al., 1976), and Raman spectroscopy (Mendelson, 1976), as well as time-resolved polarized fluorescence measurements (Chen et al., 1977; Heyn, 1979; Jähnig, 1979; Kawato et al., 1977; Wolber and Hudson, 1981), primarily reflects the time scale over which the experimental averaging occurs. Discrepancies between order parameter values determined from nanosecond and microsecond ranges suggest slow dynamic motions occurring within the bilayer and have been rationalized as fatty acyl-chain motions occurring at rates of 10^{-7} to 10^{-8} s, within the lipid matrix. Differences between NMR and fluorescence averaging times are irrelevant if intermediate relaxation processes (with $\phi \gg \tau_{FL}$ but $\phi \ll \tau_{NMR}$) are absent.

Traditionally dynamic fluorescence studies of lipid bilayers have been restricted to the nanosecond time regimen, and the submicrosecond time "window" has not been explored in any great depth by this spectroscopic technique. As such, possible slower relaxation processes with $\phi \gg \tau_{FL}$ are not detected. Experiments discussed here focus on examining gel-fluid lipid exchange rates occurring on the submicrosecond time scale. By use of a membrane probe with a mean fluorescence lifetime ($\langle\tau_{FL}\rangle$) on the order of several hundreds of nanoseconds, the fluorescence time window can be extended to span this critical submicrosecond region. Under such conditions, the experimental averaging time ($\langle\tau_{FL}\rangle$) is now longer than the rotational correlation time (ϕ), and equilibrium is established. Now both time-resolved and steady-state fluorescence probe studies can provide a convenient tool for investigation of submicrosecond lipid acyl-chain motions.

Earlier investigations suggest that the polarized fluorescence emissions of the membrane probe coronene are influenced by slow packing fluctuations in lipid bilayers below the phospholipid T_c. The significantly longer fluorescence lifetime ($\langle\tau_{FL}\rangle > 200$ ns) of this probe provides sensitivity to lipid chain disordering events (or fluctuations) that occur well after the decay of most other fluorescence probes (Davenport et al., 1986, 1988). Coronene represents an anisotropic rotor capable of both in-plane and out-of-plane rotations. However, as a direct result of its unique disk-like planar symmetry (D_{6h}), the in-plane principal transition probabilities are equal (Jablonski, 1950; Zimmerman and Joop, 1961) and thus are averaged over the plane of the molecule (Michl and Thulstrup, 1986). As a consequence, in-plane rotational motions are not possible to detect in the fluorescence polarizaton experiment, and consequently only out-of-plane motions will be observed, as discussed previously for coronene dispersed in long-chain alkane matrices (Lamotte and Joussot-Dubien, 1974; Lamotte et al., 1975). This results in a limiting anisotropy value of $r_0 = 0.1$. This value has been demonstrated experimentally for coronene rotationally restricted in frozen ethanol (Zimmerman and Joop, 1961). In the following, observed depolarizing motions of coronene within lipid bilayers will thus depend upon out-of-plane rotations ($\langle r_{op}\rangle$) only.

Previous lipid dynamic studies using long-lived fluorescence probes (for a review see Davenport and Targowski, 1995) have been described by Ruggiero and Hudson (1989) using *trans*-parinaric acid, and Sassaroli et al. (1993) using the intramolecular excimeric probe di-(1′pyrenedecanoyl)-phosphatidylcholine (dipy$_{10}$PC). In the former study, the amplitude of the long-lifetime component (30–50 ns) is assigned to probes residing in the gel phase lipid and reveals a strong temperature dependence characteristic of critical fluctuations. In the latter investigation, reduced volume fluctuations occurring on a time scale of 10^{-7} s are observed with increased applied hydrostatic pressure (preliminary hydrostatic pressure studies using coronene suggest similar behavior; Davenport and Targowski, 1993).

In the following, we present experimental analyses of time-resolved fluorescence emission anisotropy data obtained for the long-lived fluorescence membrane probe coronene embedded in DPPC SUV bilayers, using two heterogeneous dynamic lipid bilayer models. Whereas a single discrete exchange or lipid "melt" rate between "gel" and "fluid" lipid regions is defined for a compartmental model, a "gated" distribution of such lipid "melt" or exchange rates is assumed for the distributional model. Here, using appropriately derived data fitting functions, which define the compartmental or distributional models, quantitative information about submicrosecond gel-fluid exchange rates has been directly resolved. These spectroscopically derived thermodynamic values are compared with those previously determined using differential scanning calorimetry (DSC) and ultrasound studies of similar bilayer systems. Preliminary accounts of portions of this work have been presented elsewhere (Davenport et al., 1988; Targowski et al., 1992).

THEORY

Compartmental model

Three coexisting lipid phases (or compartments) are broadly defined: gel (G), fluid (F), and an additional immobilized

lipid fraction (N). The fluorescence membrane probe (in this case coronene) is assumed to distribute nonpreferentially into all lipid phases with the same average fluorescence lifetime, τ_{FL}, in all phases (i.e., nonassociative model). Gel and fluid lipid regions are in equilibrium on the submicrosecond time scale, and exchange between these phases is defined by the exchange rates k_{GF} (for F→G) and k_{FG} (for G→F) and the rate equations

$$\frac{dF}{dt} = -k_{GF} \cdot F + k_{FG} \cdot G \tag{1}$$

$$\frac{dG}{dt} = -k_{FG} \cdot G + k_{GF} \cdot F,$$

where F and G are defined as the number (concentration) of lipids of each fraction. The lipid phases defined here are independent of Gibbs' phase rule, as discussed previously by Lee (1977) for membrane systems.

The equilibrium conditions

$$\frac{dF}{dt} = 0 \quad \text{and} \quad \frac{dG}{dt} = 0 \tag{2a}$$

lead to the relationship between k_{FG} and k_{GF}:

$$k_{GF} \cdot F = k_{FG} \cdot G. \tag{2b}$$

The immobilized gel fraction, excluded from the equilibrium, results on this time scale in a nonexchangeable lipid fraction N (Fig. 1 *A*). Rotational motions of embedded coronene probes in the fluid, gel, and nonexchangeable lipid fractions are represented by ϕ_F, ϕ_G, and ϕ_N, respectively. However, it is assumed that rotational rates of the probe in both the exchangeable and nonexchangeable gel fractions are identical, i.e., $\phi_G = \phi_N$.

The depolarizing behavior of probes embedded in the lipid phases (F) and (G) will depend on the evolution of their surroundings. Three limiting cases may be described.

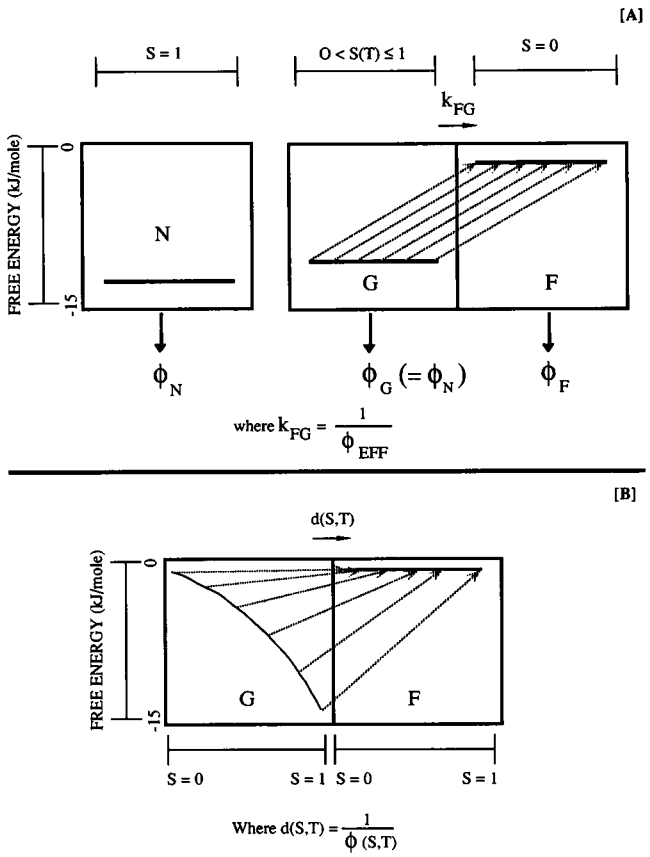

FIGURE 1 Schematic representations of (*A*) the compartmental and (*B*) the distributional models. For the compartmental model, three lipid compartments are defined by limiting order parameters and associated free energies of the system: a nonexchangeable fraction (N), where lipid does not melt appreciably on the submicrosecond time scale and included probes do not undergo any rotational motions ($S \rightarrow 1$) until very close to T_c; the fluid (F) lipid (where $S \rightarrow 0$) and embedded probe molecules are free to rotate; the gel (G) region (where $0 < S(T) \leq 1$). Regions F and G are in equilibrium on the submicrosecond time scale. Lipid melting may be defined by a discrete gel-fluid exchange rate (k_{FG}), which results in a single (effective) rotational time (ϕ_{EFF}) for the embedded fluorescence probe. In contrast, for the distributional model the free energy of the gel lipid phase (G) is described by the Landau free energy expansion (dependent on both temperature and order parameters). Consequently, melting of the lipid is now described by a distribution of lipid exchange rates ($d(S,T)$) and hence probe rotational rates ($\phi(S,T)$).

Case 1

Fluorescence probes that remain in their original lipid environment over all time are needed for probe depolarization. Their contribution, assuming no back phase transfer of the probe, to the decay of $r(t)$ may be expressed as

$$r_{F_0}(t) = \beta_F \cdot e^{-k_{GF} \cdot t} \cdot e^{-t/\phi_F} \tag{3a}$$

$$r_{G_0}(t) = \beta_G \cdot e^{-k_{FG} \cdot t} \cdot e^{-t/\phi_G},$$

where the probe fractions for each lipid compartment may be represented as

$$\frac{\beta_F}{r_0} = \frac{F}{F+G+N} \quad \frac{\beta_G}{r_0} = \frac{G}{F+G+N} \quad \frac{\beta_N}{r_0} = \frac{N}{F+G+N}. \tag{3b}$$

Case 2

The second case is one in which the lipid surroundings of probes undergo one gel or melting transition F→G or G→F, respectively, in a time t' from excitation. In this case the contribution to the expression for $r(t)$ should be calculated from the convolution of initial decay in the range 0 to t', and the final decay in the range t' to t. Consider, for

example, probes initially in phase F. The fraction of probes whose environment undergoes the transition from F to G in the time period t' to $(t' + dt')$, according to Eqs. 1 and 3a, is

$$\left(\frac{F}{(F+G+N)}\cdot e^{-k_{GF}t'}\right)\cdot k_{GF}\cdot dt',$$

and the decay of their initial anisotropy is within the same time period. After this, until time t, the probe rotates within phase G with correlation time ϕ_G. Combining these processes, we can write

$$r_{F_1}(t) = \int_0^t (\beta_F\cdot e^{-k_{GF}t'})\cdot k_{GF}\cdot e^{-t'/\phi_F}\cdot e^{-(t-t')/\phi_G}\cdot dt'$$

$$= \int_0^t r_{F_0}(t')\cdot k_{GF}\cdot e^{-(t-t')/\phi_G}\cdot dt',$$

and by analogy,

$$r_{G_1}(t) = \int_0^t (\beta_G\cdot e^{-k_{FG}t'})\cdot k_{FG}\cdot e^{-t'/\phi_G}\cdot e^{-((t-t')/\phi_F)}\cdot dt'$$

$$= \int_0^t r_{G_0}(t')\cdot k_{FG}\cdot e^{-(t-t')/\phi_F}\cdot dt'.$$

Integration gives

$$r_{F_1}(t) = \beta_F\cdot\frac{k_{GF}}{\phi_F^{-1}+k_{GF}-\phi_G^{-1}}(e^{-\phi_G^{-1}t} - e^{-(k_{GF}+\phi_F^{-1})t}) \quad (3c)$$

$$r_{G_1}(t) = \beta_G\cdot\frac{k_{FG}}{\phi_F^{-1}-k_{FG}-\phi_G^{-1}}(e^{-(k_{FG}+\phi_G^{-1})t} - e^{\phi_F^{-1}t}).$$

Case 3

Case 3 is the one in which probes embedded in lipid surroundings undergo more then one lipid transition. These rotational motions may be added to Case 2 only if the depolarization of probes in the fluid phase (defined by the rotational correlation time ϕ_F) is much shorter then any other depolarizing process. Under such conditions, the probe when embedded in the fluid phase (before or after the lipid phase change) will undergo fast rotations and be completely depolarized. Hence subsequent lipid transitions have no influence on the orientational correlation of the probe.

Probes embedded in the nonexchangeable gel fraction (N) contribute to the decay of $r(t)$ in a simple way:

$$r_N(t) = \beta_N e^{-\phi_N^{-1}t}. \quad (3d)$$

Combining all of the above limiting cases discussed (Eqs. 3a–3d), the total decay of the emission anisotropy, $r(t)$, may be expressed:

$$r(t) = \left[-\beta_G\cdot\frac{k_{FG}}{\phi_F^{-1}-k_{FG}+\phi_G^{-1}} + \beta_F\left(1-\frac{k_{GF}}{\phi_F^{-1}+k_{GF}-\phi_G^{-1}}\right)e^{-k_{GF}t}\right]e^{-\phi_F^{-1}t} \quad (4)$$

$$+\left[\beta_F\cdot\frac{k_{GF}}{\phi_F^{-1}+k_{GF}-\phi_G^{-1}} + \beta_G\cdot\left(1+\frac{k_{FG}}{\phi_F^{-1}-k_{FG}-\phi_G^{-1}}\right)e^{k_{FG}t}\right]e^{-\phi_G^{-1}t} + \beta_N e^{-\phi_N^{-1}t}.$$

This expression may now be simplified because

$$\frac{1}{\phi_F} \gg \left(k_{FG}, k_{GF}, \frac{1}{\phi_G}, \frac{1}{\phi_N}\right), \quad (5)$$

and the rotational motions of the probe in gel (G) and immobilized (N) fractions may be assumed to be the same (i.e., $\phi_G = \phi_N$). Equation 4 thus simplifies to

$$r(t) = \beta_F\cdot e^{-t/\phi_F} + (\beta_G\cdot e^{-k_{FG}t} + \beta_N)e^{-t/\phi_N}. \quad (6)$$

Consequently, in addition to two real rotational correlation times ϕ_F and ϕ_N observed for the probe, one more effective rotational time, which is equivalent to the exchange rate between gel and fluid lipid, may be extracted from the experiment ($\phi_{EFF} = 1/k_{FG}$). It is pertinent to note that only a single gel-fluid exchange rate (k_{FG}) exists in Eq. 6, and equilibrium between gel and fluid phases defines a reversible exchange of G $\rightleftharpoons$ F. This arises from an irreversible transfer of fluorescence probes from G to F, carrying information about the luminescence excitation direction, and is a result of the conditions described in Eq. 5.

At temperatures well below the lipid phase transition, the lipid is presumed to be predominantly gel-like. Under such conditions coronene molecules are essentially immobile ($k_{FG} \rightarrow 0$; $\beta_F \rightarrow 0$), and values for ϕ_N are expected to be dominated by whole vesicle rotation and represented by a residual anisotropy term (r_∞). Interestingly, $(\beta_G + \beta_N)$ defines the r_∞ term commonly observed from time-resolved fluorescence emission anisotropy (EA) measurements of the more common shorter lived fluorescence membrane probes (e.g., 1,6-diphenyl-1,3,5-hexatriene, DPH) (Chen et al., 1977; Kawato et al., 1977; Heyn, 1979; Lakowicz et al., 1979; Davenport et al., 1986), anthroyloxy fatty acids (Vincent et al., 1982), perylene (Lakowicz and Knutson, 1980), and parinaric acid (Wolber and Hudson, 1981) when embedded in membranes.

Distributional model

In contrast to the compartmental model, where lipid exists as gel (ordered) or fluid (disordered) phases, in this alternative model a distribution of gel-fluid lipid melting (or

fluctuation) rates ($d(S,T)$) is embedded in the expression for the time-resolved fluorescence EA (Fig. 1 *B*). This arises directly from the corresponding distribution of lipid ordering within the bilayer. The order parameter used here (S) is defined as the average conformational order over all -CH_2- segments (n) along the fatty acyl chain of a phospholipid ($S = N^{-1}\Sigma_n(S_n)$ and $S_n = [(3\langle\cos^2\theta_n\rangle - 1)/2]$, where N is the total number of methylene segments (Seelig and Seelig, 1974b; Brown and Seelig, 1979; Jähnig, 1981a). The instantaneous orientation of a segment n is described by the angle (θ_n) between its direction and the preferred direction, i.e., the membrane normal. It is important to note that the order parameter (S) used here relates to conformational ordering associated with the lipid acyl chains, in contrast to the second rank order parameter [$\langle P_2\rangle = (3\langle\cos^2\beta\rangle - 1)/2$] determined from the second Legendre polynomial describing the orientational distribution probability function, $f(\beta)$, defined for fluorescent probes with cylindrical symmetry embedded within lipid bilayers (Kawato et al., 1977; Kooyman et al., 1983; Wang et al., 1991). In the distributional model we have allowed possible order parameters to lie in the range $0 \leq S \leq 1$. Here $S = 1$ indicates complete system ordering with fatty-acyl chains (all-*trans*) aligned with the membrane normal. For DPPC in the gel ($L_{\beta'}$) all-*trans* phase, where hydrocarbon chains are tilted around 27° (Chapman et al., 1967) to the bilayer normal, $S_{gel} \approx 0.7$. Negative values for S have been excluded (although they are possible for individual (S_n) methylene segments in the *gauche* conformation) (Seelig and Seelig, 1974). Under conditions of negative S values, all acyl chains of the phosphoglyceride molecules will orient more parallel with the membrane surface. This appears an unlikely situation because of extensive hydrophobic acyl chain interactions. With this degree of macroscopic disordering, the integrity of the bilayer structure is jeopardized. Thus a more physiologically relevent lipid order parameter range of $0 \leq S \leq 1$ was employed in these studies.

The distributional model is adapted from Landau theory describing gated fluctuations and is based on reviews by Jähnig (1981a), combined with precise energy shapes determined previously by Mitaku et al. (1983) for DPPC SUVs using ultrasound studies. To achieve lipid melting, a certain activation energy ($E_{ACT}(S,T)$) must be achieved, proportional to the difference in the free energy (F) of the lipid molecule when in gel-like ($F(S,T)$) and fluid-like ($F(S = 0,T)$) phases:

$$E_{ACT}(S,T) = F(S = 0,T) - F(S,T). \tag{7}$$

In analogy with diffusion arguments discussed by Jähnig (1981a), an effective rotational rate, ($d(S,T)$ or, alternatively, $\phi(S,T)^{-1}$), for the embedded fluorescence probe is associated with the same activation energy barrier. The hydrocarbon chains of the lipid matrix surrounding the fluorescence probe must undergo sufficient packing density fluctuations for rotational motion of the probe to occur. It is expected that some multiple (or gating function, γ) of the activation energy barrier (i.e., simultaneous melting of several lipid molecules) will actually permit probe rotation. Consequently, the activation energy ($E_{ACT}(S,T)$) serves to link both thermodynamic quantities describing the heterogeneously packed lipid bilayer together with spectroscopic dynamic parameters derived from fluorescence EA measurements.

$$\frac{1}{\phi(S,T)} \sim e^{-\gamma(E_{ACT}/RT)}. \tag{8}$$

At equilibrium, according to Landau theory (Landau and Lifchitz, 1958), the free energy (F) of a given system can be expanded in powers of the conformational order parameter S ($0 \leq S \leq 1$):

$$F(ST) = -A_1S + \frac{1}{2}A_2S^2 - \frac{1}{3}A_3S^3 + \frac{1}{4}A_4S^4\ldots, \tag{9}$$

where A_2 is linearly related to temperature, $A_2 = a(T - T^*)$, and T^* is the pseudocritical temperature. T^* is related to the measured lipid phase transition temperature T_c in a simple way (Jähnig, 1981a; deGennes and Prost, 1993) through the Landau coefficients:

$$T^* = T_c - \frac{2A_3^2}{9aA_4}. \tag{10}$$

Under conditions of constant membrane surface pressure, $A_1 = 0$. The Landau coefficients (a, A_3, A_4) and T^* are derived from thermodynamic quantities, explicitly determined previously for DPPC unilamellar vesicles (ULVs) by Mitaku et al. (1983) from ultrasound studies. Although the Landau free energy expansion applies specifically to second-order transitional behavior ($A_3 = 0$ and $T^* = T_c$), because the gel-fluid phase transition for lipid systems is described as only weakly first order, this free energy expansion still applies ($A_3 \neq 0$ and $T^* < T_c$).

A normalized Boltzmann distribution defines the probability ($P(S,T)$) of an ensemble of molecules with a particular activation energy ($E_{ACT}(S,T)$) with order parameter S:

$$P(S,T) = \frac{\exp\left(-\dfrac{E_{ACT}(S,T)}{RT}\right)}{\displaystyle\int_0^1 \exp\left(-\frac{E_{ACT}(S,T)}{RT}\right)dS}. \tag{11}$$

At temperatures well below the lipid transition temperature (T_c), the activation energy ($E_{ACT}(S,T)$) required for melting is large and the corresponding probability of lipid fluidization is low. As expected, lipid ordering decreases strongly with increasing temperature, whereas the probability increases.

Correspondingly, at temperatures close to T_c ($E_{ACT}(S,T) \rightarrow 0$), the effective rotational rate ($d(S,T)$) of the probe in the lipid bilayer becomes limiting and order indepen-

dent:

$$d(S,T \approx T_c) = d_\infty(T). \quad (12)$$

Alternatively, for any $T \leq T_c$,

$$d(S = 0,T) = d_\infty(T). \quad (13)$$

Thus values of $d_\infty(T)$ reflect temperature-dependent rates of rotation achieved by the probe as if embedded in a "pure" isotropic solvent with microviscosity properties corresponding to those of the surrounding fluid-like (F) lipid:

$$d_\infty(T) \approx \frac{1}{\phi_F(T)}. \quad (14)$$

Effective rotational rates for the probe (from Eqs. 8 and 12–14) may thus be expressed:

$$\frac{1}{\phi(S,T)} = d_\infty(T) \cdot e^{-\gamma E_{ACT}(S,T)/RT}. \quad (15)$$

By linking the effective rotational rates ($d(S,T)$, Eqs. 13 and 14) of the fluorescence probe with the probability ($P(S,T)$, Eq. 11) of a lipid effectively fluidizing, through the activation energy at a particular orientational order parameter (S, where $0 \leq S \leq 1$), the time-resolved fluorescence EA decay function may now be predicted:

$$r(t) = r_0 \int_0^1 P(S,T) \cdot e^{-d(S,T)t}\, dS \quad \text{where} \quad d(S,T) = \frac{1}{\phi(S,T)}. \quad (16)$$

Nonlinear least-squares fits of this expression to time-resolved polarized data obtained for fluorescence probes embedded in bilayers result in the retrieval of values for the gate function (γ) and the limiting diffusion rate (d_∞). The five coefficients (A_1–A_4 and T_c) that serve to precisely define the free energy versus temperature profile are fixed in the analysis; only γ and d_∞ are allowed to vary. As for the compartmental model, it is assumed that the average fluorescence lifetime of the probe is independent of the lipid phase (i.e., nonassociative modeling).

It is pertinent to note that this expression is independent of the nature of the fluorescence probe and dependent only on inherent thermodynamic properties of the phospholipid, unlike previous homogenous "probe" distributional models, which have focused within their formalism on the angular distributions and symmetry of the probe molecule itself (Heyn, 1979; Jähnig, 1979; Kawato et al., 1977; Zannoni, 1981). In the model discussed here, a heterogeneous population of probe molecules reflecting the heterogeneous lipid environment is assumed, and no hindering potential is imposed upon the rotational motions of the probe when it is partitioned within either the gel or the fluid environment, as a direct result of the long experimental averaging regime over which the experiment is conducted, i.e., $r_\infty \rightarrow 0$ when $t \rightarrow \infty$. Thus, in principle, this general expression is applicable to the analysis of time-resolved fluorescence EA decay profiles of fluorescence probes embedded in lipid bilayers, where depolarizing probe motions arise as a direct result of lipid fluctuations. Obviously, anisotropic rotational motions observed for planar dyes with lower symmetry (as observed for perylene, D_{2h}), e.g., fast in-plane "slipping" motions combined with slower out-of-plane rotations (Lakowicz and Knutson, 1980; Brand et al., 1985), or probe rotations arising from a possible subensemble oriented between the bilayer lipid leaflets and parallel with the membrane surface (van der Heide et al., 1996), both of which are presumed to be less dependent on direct lipid fluctuation effects, are not included in the models proposed here.

Further refinements may be made of the model, including adjustment of the required $F(S,T_c)$ for melting, corresponding to the gate threshold, or alternatively, multiple d_∞ values in the $F(S,T_c)$ versus rotational $d(S,T)$ rates. In addition, the effects of applied hydrostatic pressures on lipid fluctuations may be included in this model by modification of the Landau free energy expansion (Davenport and Targowski, 1993; Davenport et al., 1995).

MATERIALS AND METHODS

Preparation of samples

L-α-Dimyristoylphosphatidylcholine (DMPC) and L-α-dipalmitoyl-phosphatidylcholine (DPPC) were purchased from Sigma Chemical Company (St. Louis, MO) and used without further purification. Purity was judged by single-spot thin-layer chromatography analysis, using silica gel G plates (Universal Scientific, Atlanta, GA) and chloroform:methanol:water (65:25:4, v/v/v) as the developing solvent. Spot identification was by phosphorus staining reagent (Dittmer and Lester, 1964) and charring (2% sulfuric acid in methanol by volume). DPH and high-performance liquid chromatography (HPLC)-purified coronene were purchased from Molecular Probes (Eugene, OR) and used as supplied.

Small unilamellar vesicles (SUVs) of DMPC or DPPC were prepared by sonication using an ultrasonic probe (Heat Systems; Ultrasonics) in 0.01 M Tris (tris (hydroxymethyl)aminomethane)-HCl containing 0.1 M sodium chloride (pH 8.5) at 35°C and 55°C, respectively, well above the respective phospholipid phase transition temperatures (Melchior and Steim, 1976). Lipid samples were flushed continuously with nitrogen to minimize any lipid peroxidation (Hauser, 1971; Brunner et al., 1976). Separation of single-bilayer vesicles was achieved by ultracentrifugation (Beckman Airfuge; Beckman Instruments, Palo Alto, CA) at 100,000 × g for 60 min at room temperature, essentially according to the method of Barenholz et al. (1977). The uppermost fraction of the supernatant containing SUVs was isolated. Large unilamellar vesicles (LUVs) were prepared using an extruder (Lipex-Biomembranes, Vancouver, BC, Canada) equipped with a thermostatted temperature jacket and a 0.1-μm extrusion membrane. Lipid samples were cycled through the extruder at least three times and freeze-thawed between extrusions using liquid nitrogen, essentially as described elsewhere (Hope et al., 1985). After preparation, all unilamellar vesicles (ULVs) were maintained above their respective T_c and used immediately for spectroscopic analyses. Samples were discarded within 3 days of preparation. Lipid phosphorus was determined according to the method of McClare (1971). Total phospholipid concentrations used for fluorescence measurements were typically 0.2 mM.

Vesicles used for steady-state fluorescence studies were labeled using either coronene or DPH by direct solvent injection (Chen et al., 1977) from stock solutions in tetrahydrofuran (2 mM and 1 mM, respectively). Labeling of ULVs with DPH was achieved by stepwise addition from a microsyringe into a vortexing suspension (3 ml) of ULVs (1 mM total phospholipid) to give a final probe concentration that was never greater

than 2 μM. Labeled suspensions were incubated at temperatures greater than T_c for the lipid for approximately 2 h to ensure complete uptake of the fluorescent dye, as judged by the observation that there was no further increase in fluorescence intensity with time (Davenport et al., 1985). Any tetrahydrofuran added during the labeling procedures was removed by evaporation using a gentle stream of nitrogen gas. For coronene-labeled ULVs a nominal probe-to-phospholipid molar labeling ratio of 1:200 was employed. Lipid samples were incubated overnight, above T_c, using gentle swirling to allow maximum penetration of the dye into the membrane. Removal of any unincorporated coronene existing as aggregates was achieved by passing the ULVs down a PD-10 Sephadex G-25 M column (height 5 cm; i.d. 1.2 cm; void volume 9 ml; Pharmacia, Uppsala, Sweden) using the standard Tris buffer as the running solvent (0.2 ml·min^{-1}). Vesicle fractions labeled with coronene were eluted with the void volume and identified by correspondence of the scatter and fluorescence peaks. Fractions were pooled and ULVs stored above their respective phase transition temperatures.

SUVs used for time-resolved measurements were prepared by cosonication of the phospholipid with the appropriate concentration of coronene, to give a molar labeling ratio of 1:200 (probe to phospholipid). Before sonication, the lipid and dye were vacuum dessicated for up to 12 h to remove any traces of organic solvent.

In all cases, vesicle samples with no fluorescent dyes were prepared as described above and used to assess background vesicle scatter for the equivalent phospholipid concentration, which was subsequently subtracted from the corresponding spectroscopic data. The background due to vesicles was typically less than 0.2% of the total signal. Furthermore, for all fluorescence measurements, inner filter effects were obviated (Parker and Rees, 1962) by ensuring that the total absorption of the samples (arising from both the dye and vesicle scatter) at the wavelength of excitation was always less than 0.1.

Fluorescence measurements

Steady-state fluorescence excitation and emission spectra were obtained using a Perkin-Elmer LS-50B spectrofluorimeter (Norwalk, CT) operating in the ratio mode to eliminate source intensity fluctuations. The temperature of the lipid samples was achieved using a water-circulating thermostatted cuvette holder with continuous feedback to an external solid-state relay (Omega Engineering, Stamford, CT) connected to a water bath, and reporting the experimental temperature conditions directly to a controlling personal computer (80386SX). Measurement of steady-state emission anisotropies and total fluorescence intensities were essentially as described in detail elsewhere (Chen et al., 1977). Briefly, steady-state polarized emission intensities were obtained using Polacoat dichroic film polarizers (Sterling Optics, Williamstown, KY) oriented either vertically or horizontally in the excitation and observation paths. Excitation and emission wavelengths used for coronene were 340 nm and 448 nm, respectively, and 355 nm and 430 nm, respectively, for DPH. Excitation and emission bandwidths were typically each 4 nm. The steady-state emission anisotropy, $\langle r \rangle$, was calculated from

$$\langle r \rangle = \frac{G \cdot I_{VV} - I_{VH}}{G \cdot I_{VV} + 2I_{VH}}, \tag{17}$$

where $G = (I_{HH}/I_{HV})$ and represents a correction factor for the inequality of sensitivity of the detection system to horizontally and vertically polarized emissions. The first subscript, V or H, refers, respectively, to the vertical or horizontal orientation of the dielectric vector of the excitation and the second to those for emission. Automated acquisition of lipid "melt" profiles of $\langle r \rangle$ versus increasing temperature (typical scan interval of 2.5°C) was controlled by an 80386SX personal computer running noncommercial PASCAL software developed in this laboratory.

Time-resolved fluorescence spectroscopy

Nanosecond time-resolved fluorescence decay data were collected using a home-built, computer-controlled single photon counting spectrofluorometer, essentially as described elsewhere (Badea and Brand, 1979). Sample excitation was achieved using an IBH (System 5000) thyratron-gated, nitrogen-filled flashlamp (IBH Consultants, Glasgow, Scotland) running typically at 35 kHz repetition rate, 0.7 mm electrode gap, and 0.75 atm nitrogen pressure. Under these conditions, bright light pulses, typically 3 ns full width half-maximum (FWHM), were obtained. Emitted photons were detected using a Philips XP-2020Q photomultipier tube (Slatersville, RI). Fluorescence decay profiles were collected contemporaneously along with blank vesicle samples and an excitation profile $E(t)$, obtained using a dilute scattering solution of Ludox HS-30 (DuPont, Wilmington, DE) and used for deconvolution of the data. Excitation of the coronene-labeled vesicle samples was accomplished using a 340-nm interference filter (12-nm bandpass; Ealing-Electro Optics, Holliston, MA). The fluorescence-emitted photons were isolated using a Jobin-Yvon holographic grating (1200 grooves/mm) H-10 monochromator (Instruments SA, Metuchen, NJ). Emission bandwidths of 16 nm (2-mm slits) were used for the lipid samples. For polarized decay measurements, a rotating polarizer was used in the excitation pathway, with a fixed polarizer oriented vertically in the emission train. A timing calibration of 0.4 ns/channel was used. Because of the long fluorescence lifetime of coronene in vesicles, polarized total intensity ($S(t)$) decay profiles (Eq. 18), typically collected over not less than 512 channels (and in some case 800 channels), were truncated. Truncation of difference decay profiles ($D(t)$) was only observed at low temperatures. Recovered model parameters were not significantly affected by data truncation. However, determination of the instrumental "G" or grating factor (Chen and Bowman, 1963) and steady-state emission anisotropy values for the lipid systems described were achieved by extending the region of interest of the 918A-multichannel buffer (EG&G Ortec, Oak Ridge, TN) to cover 2048 channels. Collected photon counts were integrated for 100 s over this time window for each polarized decay component.

The time shift between excitation and emission wavelengths (Lewis et al., 1973; Wahl et al., 1974) and reproducibility of a single exponential decay was achieved from the same experiment using 9-cyanoanthracene in HPLC-grade methanol ($\tau_{FL} \approx 11.8$ ns; air saturated) as a standard, with a vertical polarizer in the excitation path and corresponding "magic angle" emission optics (polarizer oriented 55° to the vertical). All other excitation and emission conditions used were identical. Temperature control was achieved as described for steady-state measurements and automated for acquisition of time-resolved lipid "melt" profiles.

Analysis of the decay data

Single-curve analyses of time-resolved polarized decay profiles were achieved after subtraction of the appropriate blank vesicle contribution, ensuring that correct statistical weights were used for the subsequent analyses, as discussed previously by Barkley et al. (1981).

Polarized fluorescence decay data were analyzed as described elsewhere (Chen et al., 1977). Briefly, for each data set, sum ($S(t)$) and difference ($D(t)$) decay profiles were constructed from the experimental data as

$$\begin{aligned} S(t) &= G \cdot I_{VV}(t) + 2I_{HV}(t) \\ D(t) &= G \cdot I_{VV}(t) - I_{HV}(t). \end{aligned} \tag{18}$$

Theoretical decay profiles (or impulse response functions), $\sigma(t)$ and $\delta(t)$, were convolved onto the experimentally derived excitation profile $E(t)$ and fitted to Eq. 18 via a nonlinear least-squares search as described by Brandt (1970). For the multiexponential time decay analysis,

$$\begin{aligned} S(t) &= E(t) \otimes \sigma(t) = E(t) \otimes \sum_j \alpha_j e^{-(t/\tau_j)} \\ D(t) &= E(t) \otimes \delta(t). \end{aligned} \tag{19}$$

Two separate analyses of the experimental difference decay curves, $D(t)$, were performed according to the compartmental or distributional models.

In both cases the decay of the total emission, $\sigma(t)$, is assumed to be the same for all kinetic components of the emission anisotropy decay, i.e., a nonassociative lifetime model was adopted (Chen et al., 1977; Beechem et al., 1984) and the total intensity decay parameters were fixed for the difference decay analyses performed.

For the compartmental model,

$$\delta(t) = \left(\sum_i \beta_i e^{-t/\phi_i} \right) \cdot \sigma(t), \tag{20}$$

and i represents a subpopulation of probes located in a particular rotational environment as discussed above (see Theory).

For the distributional model (Eq. 16), the impulse response can be written

$$\delta(t) = \left(r_o \int_0^1 P(S,T) e^{-d(S,T)t}\, dS \right) \cdot \sigma(t). \tag{21}$$

By the use of nonlinear least-squares fitting, retrieved fitted parameters (β and ϕ for the compartmental model, and γ and d_∞ for the distributional model) were judged to be acceptable from reduced χ^2 values, residuals, and their autocorrelation functions (Badea and Brand, 1979). For conditions when χ^2 is close to unity, standard deviation errors for the retrieved parameters may be extracted from their covariance matrix (Brandt, 1970). Errors presented in Figs. 4 through 6 are calculated in this way.

RESULTS

Steady-state fluorescence studies

Nonincorporated coronene aggregates adsorbed to the lipid bilayer surface were readily detected as a broad, featureless band ($\lambda_{max} \approx 580$ nm) in the emission spectrum. On passage of vesicle samples down a Sephadex G-25 M gel filtration column, this spectral signature was lost, giving the characteristic emission spectrum for coronene embedded in lipid vesicle systems (Fig. 2). Vibrational peaks were relatively insensitive to temperature effects, change in the lipid phase, or lipid type, although some thermal quenching (see below) was observed with increasing temperature (Lamotte et al., 1975). Because the fluorescence emissions of coronene are exquisitely sensitive to the presence of oxygen, the thermally associated intensity quenching might be attributed to altered membrane oxygen concentration; the solubility of dissolved oxygen in the membrane is decreased with increasing temperature (Husain et al., 1982; Tan and Ramsey, 1993). For all polarized emission data presented here, vesicle samples were fully aerated (coronene embedded in de-aerated vesicle samples exhibits strong phosphorescence) and the $S_0 \rightarrow S_3$ (Katraro et al., 1979) allowed transition (340 nm) was used for excitation. Zimmerman and Joop (1961), using coronene embedded in frozen ethanol, have shown that as expected for a molecule with D_{6h} planar symmetry, $r_0 = 0.1$ and remains constant across all excitation bands.

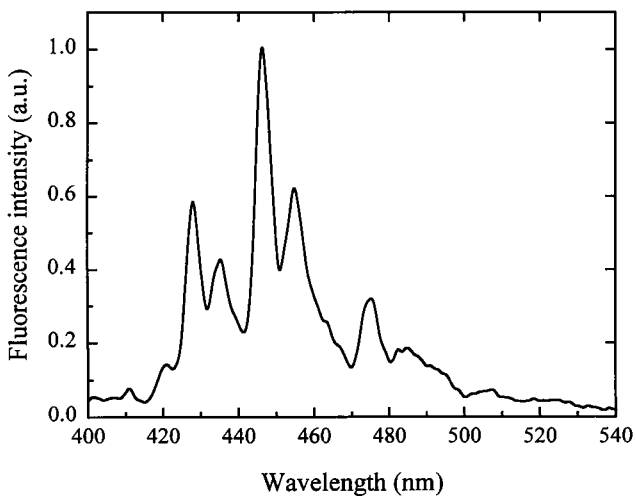

FIGURE 2 Uncorrected steady-state fluorescence emission spectrum for coronene-labeled DPPC SUVs at 35°C. A nominal molar labeling ratio for coronene to lipid of 1:200 was employed. Excitation was at 340 nm, with excitation and emission bandwidths of 4 nm each.

Steady-state fluorescence emission anisotropies ($\langle r \rangle_{op}$), as a function of increasing temperature for coronene embedded in both DPPC SUVs and LUVs, reveal "broader" lipid "melt" transition profiles than reported from the corresponding DPH-labeled samples, which are shifted to lower temperatures (Fig. 3). Such data have also been obtained previously for DMPC SUVs and/or LUVs (Davenport et al., 1988). Because of the planar symmetry of the probe and the long fluorescence lifetime (see below) of coronene in lipids, we attribute these depolarizing motions to submicrosecond lipid dynamics, which are evident at temperatures well below the normal lipid melt temperature (and the thermal pretransitional region ($L_{\beta'} \rightarrow P_{\beta'}$); Janiak et al., 1976) and are not revealed by shorter lived fluorescence probes (e.g., DPH). Furthermore, these effects were independent of vesicle size (diameter = 1000 Å and 250–300 Å for LUVs and SUVs, respectively) and hence radius of curvature.

Shifts in phase transition profiles have previously been attributed to differential partitioning of fluorescent probes into "gel" or "fluid" phases of the bilayer (Lentz et al., 1976; Thurlborn, 1981). It is not unreasonable to speculate that preferential partitioning of coronene into a more fluid lipid phase may occur here, resulting in observed anomolous lower temperature shifted "melt" transition profiles for DPPC SUVs and/or LUVs. To preclude this alternative explanation, in analogy with studies by Lentz et al. (1976), we recorded steady-state emission anisotropy profiles for coronene-labeled LUVs prepared by colyophilization of an equimolar mixture of DMPC and DPPC. Measured anisotropy values for coronene in this lipid system were a simple average of the EA values recorded in each separate lipid type, suggesting an equal distribution of probe between the two lipid phases (data not shown).

We also attempted to assess the degree of possible perturbation caused by the introduction of coronene into lipid bilayers. DPPC SUVs labeled with both coronene and DPH (1:1 with a total probe-to-phospholipid molar labeling ratio of 1:250) showed no appreciable alteration in the lipid "melt" transition curve (data not shown), as reported by DPH (under conditions of no direct excitation of coronene

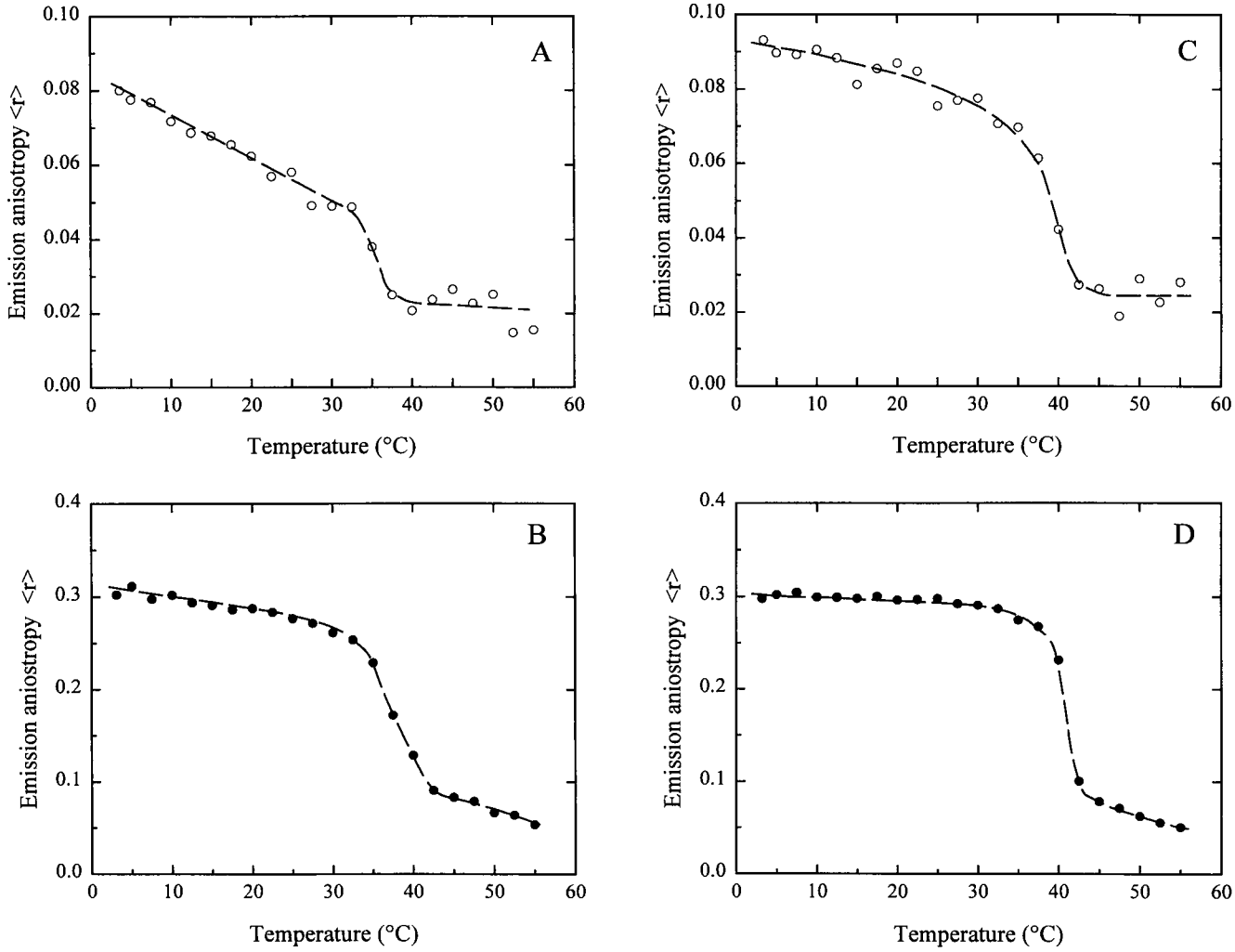

FIGURE 3 Steady-state emission anisotropy as a function of temperature for (*A*) coronene-labeled and (*B*) DPH-labeled DPPC SUVs and (*C*) coronene-labeled and (*D*) DPH-labeled DPPC LUVs. The probe-to-phospholipid molar labeling ratio used was 1:200 and 1:500 for coronene and DPH, respectively. Excitation for coronene and DPH-labeled samples was 340 nm and 360 nm, respectively, with emission recorded at 448 nm and 430 nm, respectively. Excitation and emission bandwidths were each typically 6 nm. Calculated errors were not greater than 0.005.

or energy transfer processes). Thus gross bilayer perturbations of bilayers containing coronene are not evident at probe labeling ratios typically used in lipid dynamic studies discussed here.

Time-resolved fluorescence intensity decay studies

The nanosecond time dependence of the total emission, $S(t)$, for coronene embedded in DPPC SUVs was determined at several temperatures below and up to the lipid phase transition temperature. Fig. 4 summarizes the results. Decay data at all temperatures were best fitted using three exponential components, plus a scattering component. The major decay component (τ_1), comprising essentially 98% ($\alpha_1\tau_1/\Sigma_{i=3}\alpha_i\tau_i$) of the total emission observed, appeared somewhat sensitive to temperature, resulting in a lifetime quenching from 250 to 170 ns, corresponding to an increase in temperature from 7°C to 41°C. In contrast, other recovered decay parameters ($\tau_2 \approx 37 \pm 5$ ns and $\tau_3 \approx 2 \pm 1$ ns) appear to be temperature invariant. In some cases recovery of the short-lifetime component was unreliable, and for subsequent analyses of the rotational motions of coronene in vesicles, this lifetime component was often fixed to a reasonable average value of 2.0 ns. Multicomponent lifetime decays of fluorescent dyes embedded in lipid vesicles have previously been observed for other, more well-known short-lived fluorescence membrane probes (e.g., parinaric acid: Wolber and Hudson, 1981; perylene: Lakowicz and Knutson, 1980; and DPH: Chen et al., 1977; Davenport et al., 1986). For DPH, the physical origins of this second decay component have been studied in detail by several investigators and have been attributed to a *cis-trans* photoisomerization (Lunde and Zechmeister, 1954) or excited-state species (Wang et al., 1991). In the case of coronene, the origins of the multicomponent decay profile are unclear and may arise from the

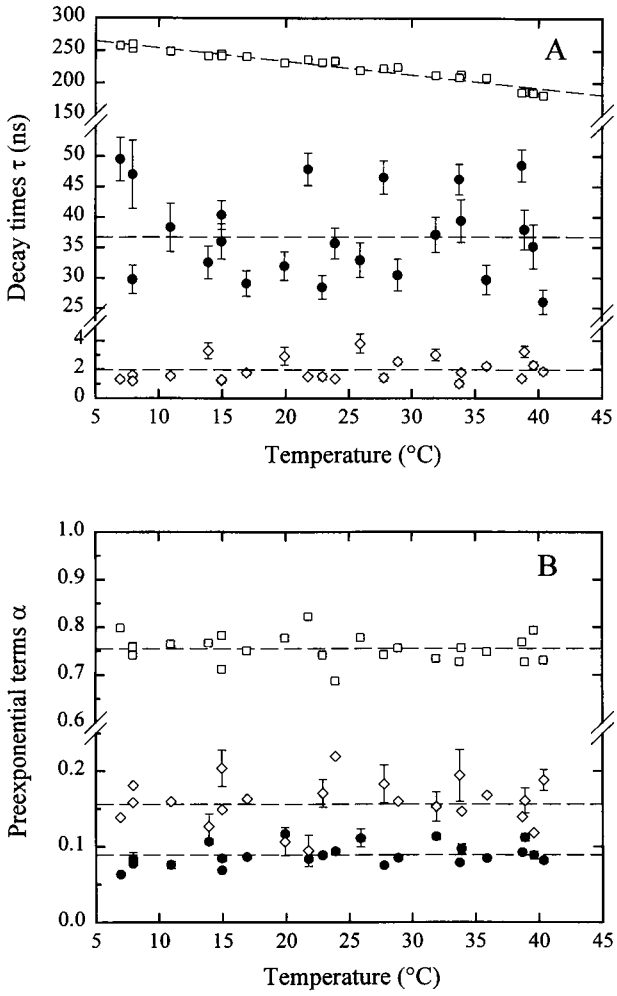

FIGURE 4 Summary of lifetime decay parameters for coronene labeled DPPC SUVs, as a function of temperature. (*A*) Fluorescence decay times: τ_1 (□); τ_2 (●); τ_3 (◇). (*B*) Preexponential terms normalized according to $(\alpha_i\tau_i/\Sigma_{i=3}\alpha_i\tau_i)$: α_1 (□); α_2 (●); α_3 (◇). Excitation was accomplished using a 340-nm interference filter (bandwidth = 12 nm), and emission was recorded at 448 nm using a 16-nm slit width. Errors not shown are within the size of the data point.

heterogeneity of probe location possibly associated with bilayer sites of varying oxygen concentration or polarity arising from variations in lipid packing and water pentration of the bilayer (Parassasi et al., 1994; Stubbs et al., 1995). In any case, the temperature invariance of the preexponential terms (α_i) (Fig. 4 *B*) associated with recovered lifetime values suggests independence of the lifetime on the gel-fluid lipid packing (i.e., there is no τ-ϕ linkage). As a consequence, a nonassociative rotational model was adopted for the lipid models. Coronene emissions in isotropic solvents, such as aerated hexane, reveal a monoexponential fluorescence decay profile with $\tau_{FL} \approx 8.0$ ns.

Time-resolved emission anisotropy decay results

Fluorescence emission anisotropy decays recorded for coronene embedded in DPPC SUVs were analyzed using either the compartmental or distributional membrane models. The data shown represent a summary of retrieved data for three separate vesicle experiments. Recovered time-resolved parameters are shown with associated standard deviation errors.

For the compartmental model, heterogeneity in probe location is assumed, and the extracted rotational correlation times (arising from exclusive out-of-plane depolarizing motions) reflect differing rotational environments within the bilayer (i.e., regions of high and low lipid order, $S \rightarrow 1$ and 0, respectively). The preexponential terms (β) represent the relative contribution of these motions at a particular temperature, with the theoretical restriction that the sum of all preexponential terms equals the limiting anisotropy value (r_0) of 0.1 (Eq. 3b).

For all temperatures examined (in the range 5–40°C) and as expected, a simple monoexponential decay law did not satisfactorily describe the polarized decay data (see Eq. 6). In general, a single correlation time plus a residual anisotropy (r_∞) term, or in some cases a double exponential decay function, best described the polarized decay data. At low temperatures, well below the phase transition temperature, a residual anisotropy term (r_∞) was clearly evident. However, with increasing temperature, a long correlation time (ϕ_N), corresponding to a nonexchangeable lipid fraction, provided equivalent or improved data fits, as judged from routine statistical criteria.

According to the compartmental model, the shorter resolved correlation time, ϕ_{EFF}, corresponds to a discrete temperature-dependent gel-fluid lipid exchange rate, k_{FG}. Values of ϕ_{EFF} range from 150 ± 40 ns at cold temperatures (hence $k_{FG} = (6.7 \pm 1.7) \times 10^6$ s at 7°C) to around 20 ns at the lipid melt transition (Fig. 5 *A*). Lipid fluctuation-induced probe rotations (arising from the exchangeable "gel" fraction (G) in our simple model) are apparent well below the lipid transition temperature for DPPC. At the lipid phase transition temperature, the "gel" lipid is predominantly melted.

Plots of the preexponential terms (β_G and β_N) associated with rotational times ϕ_{EFF} and $\phi_N = \infty$, respectively, as a function of increasing temperature show a decrease in β_N with a corresponding increase in β_G (Fig. 5 *B*). An intercept point occurs at around 23°C. Clearly, the appearance of lipid fluctuations is evident at temperatures well below T_c, their frequency increasing with increasing temperature. The expected decrease with increasing temperature of β_N, associated with the long correlation time (i.e., nonexchangeable lipid or *N* in our compartmental model), confirms a diminishing gel-like fraction.

Interestingly, the magnitude of the recovered preexponential terms ($\beta_G + \beta_N$) results in values less than the theoretically expected value of 0.1, providing evidence for at least one other rotational decay component for coronene embedded in lipid bilayers. In some analyses, we were able to extract a fast rotational correlation time ($\phi \approx 2$–5 ns). This rotational motion we ascribed to coronene in fluid or melted lipid (ϕ_F). However, ϕ_F as described by the compartmental model could not be routinely extracted from the

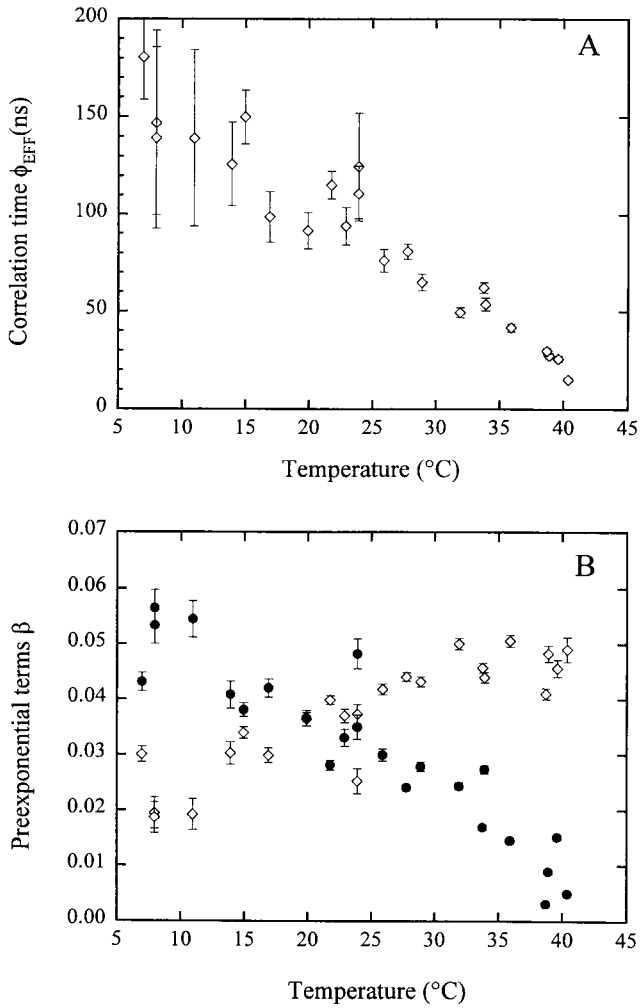

FIGURE 5 Summary of rotational decay parameters for coronene-labeled DPPC SUVs, as a function of temperature, analyzed according to the compartmental model. (*A*) Rotational correlation time, $\phi_{EFF} \equiv 1/k_{FG}$. (*B*) Preexponential factors: β_G (◇) and β_N (●). The lifetime decay parameters used for these analyses, for a given temperature, are summarized in Fig. 4. Excitation was accomplished using a 340-nm interference filter (bandwidth = 12 nm), and emission was recorded at 448 nm, using a 16-nm slit width.

data. The inability to resolve such fast rotational motions may arise directly from the timing calibration (0.4 ns/channel) used for these experiments, which was necessary because of the long fluorescence lifetime of coronene. Under these conditions the excitation pulse occupies fewer than 5 channels (FWHM) on the multichannel analyzer, and errors in resolving fast rotational decay components are not unexpected (Vecer et al., 1993). No attempt was made to correct for possible convolution artifacts introduced by using a "sparse excitation profile," because possible errors incurred would fall within those introduced by the more dominant scatter contribution from the vesicle sample. Collection of polarized decay data using two different timing calibrations with subsequent analysis by global methods (Knutson et al., 1983; Beechem and Brand, 1986) would enable overdetermination of these complicated lipid systems.

In the second case, corresponding difference decay profiles, $D(t)$, for coronene-labeled DPPC SUVs at temperatures below and up to the lipid phase transition were analyzed according to the lipid order distributional model (Eq. 16), invoking a distribution of lipid exchange rates, $d(S,T)$. As for compartmental model analyses, values of the lifetime components were first determined from constructed total intensity $S(t)$ decays (Eq. 18) obtained from measured polarized decay curves, and retrieved parameters were then fixed for subsequent difference analyses.

Although a total of seven parameters are required to fully describe the $r(t)$ expression for the distribution model (Eqs. 7–16), in practice only three factors (γ, d_∞, and r_0) serve as adjustable parameters. Values for the Landau coefficients (A_n) required to fully describe the free energy profiles for DPPC at different temperatures below the lipid phase transition, obtained previously by Mitaku et al. (1983) using ultrasound studies, were fixed in our analyses to the appropriate literature values ($A_1 = 0$; $a = 1.35$ kJ/(mol·K); $A_3 = 6.8$ kJ/mol; $A_4 = 10.1$ kJ/mol). For DPPC SUVs, a value of $T_c = 39.0$°C was used for the lipid phase transition temperature, as reported from differential scanning studies (Melchior and Steim, 1976). From Eq. 10, the pseudocritical temperature may thus be calculated ($T^* = 38.25$°C).

Fig. 6, *A* and *B*, shows, respectively, recovered values for the "gating" factor (γ) and the limiting probe diffusion rate (d_∞) as functions of increasing temperature. As reflected in the vertical error bars (representing standard deviations), there is considerable uncertainty in the parameters recovered at low temperatures far below T_c. In general, the quality of fits to the data for the two different models, as judged by χ^2 values, residuals, and autocorrelation functions, are similar for the two models. However, in contrast to fits obtained using the compartmental model, which required either a residual anisotropy term or a discrete rotational correlation rate to describe ϕ_N with varying temperature, analyses using the distributional model provided a more consistent model. Values recovered (not shown) for the freely adjustable r_0 term were around 0.07.

Values of the "gating" factor vary from around 10 at 20°C to around 5 at temperatures close to the transition (35°C). The line drawn through the data represents an arbitrary fit and is not representative of any expected theoretical relationship. The gating factor (γ) defines a multiple of the activation energy barrier that must be exceeded to permit probe rotation, i.e., the critical number of lipid molecules that must achieve "fluidization" simultaneously. Hence γ as such is indicative of a cooperative unit size of the surrounding lipid that influences the rate of rotations of the included fluorescence probe molecule. As expected, at temperatures well below T_c, the E_{ACT} barrier is large and the probability of achieving lipid fluidization is small. Values for the gate function are consequently very large, suggesting that several lipid shells (or a lipid cluster) surrounding the probe are involved in the lipid chain disordering process. With increasing temperature the cooperative nature of the lipid cluster diminishes and the gate factor tends to a lim-

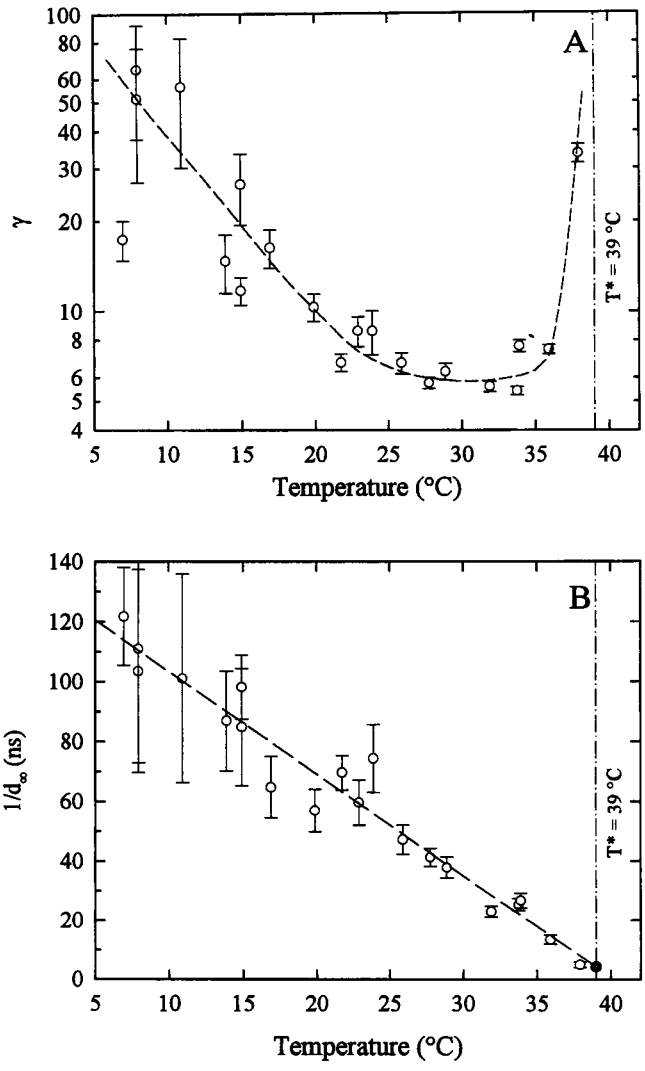

FIGURE 6 Summary of rotational decay parameters for coronene-labeled DPPC SUVs, as a function of temperature, analyzed according to the distributional model. (*A*) gate factor, γ, and (*B*) limiting diffusional rate, d_∞. The lifetime decay parameters used for these analyses, for a given temperature, are summarized in Fig. 4. Excitation was accomplished using a 340-nm interference filter (bandwidth = 12 nm), and emission was recorded at 448 nm, using a 16-nm slit width.

iting value of about 5 on approaching the lipid phase transition. However, as predicted, close to T_c, values of γ rise sharply and tend toward infinity. This arises directly from limitations of the distributional model: the free energy expansion (Eq. 9) is presumably underestimated and γ consequently overcompensates for this inadequacy. In addition, as follows from Eq. 15, the rotational rates $d(S,T)$ become independent of γ for $E_{ACT} \approx 0$, and γ may not be reliably retrieved. Consequently, the distribution model is limited to lipid fluctuations occurring below T_c in lipid bilayer membranes.

The recovered $d_\infty(T)$ terms reveal a linear dependence of the reciprocal on temperature (shown in Fig. 6 *B*), tending toward a limiting rotational rate of about 0.25 ns^{-1} at T_c (39.0°C for DPPC SUVs). The value of 0.25 ns^{-1} extracted for the limiting diffusion rate is not unreasonable for a fluorescence probe tumbling in a fluid lipid bilayer. Estimates of d_∞ may provide information on the local "microviscosity" of the immediate environment surrounding the probe.

DISCUSSION

We have sought in this study to investigate submicrosecond lipid dynamics occurring within bilayer membranes. To accomplish our aim, we have exploited the use of the fluorescent dye coronene as a hydrophobic membrane probe, where it exhibits a long mean fluorescence lifetime ($\langle\tau_{FL}\rangle \approx 200$ ns). Under such conditions, the time window of experimental observation is extended ($\tau_{FL} > \phi$), and lipid dynamics not previously detected by fluorescence methodologies may be explored. Indeed, our studies suggest that the polarized fluorescence emissions from coronene embedded in lipid bilayers are influenced by slow (submicrosecond) acyl-chain packing fluctuations. Because of the symmetry of this probe (D_{6h} planar symmetry; $r_o = 0.1$), depolarizing motions of coronene are exclusively to out-of-plane rotations. Consequently, $\langle r\rangle = \langle r\rangle_{op}$.

As with all extrinsic fluorescence probe experiments, concerns about probe location and possible perturbation effects within the lipid bilayer arise. The hydrophobic nature of coronene, combined with its inaccessibility to quenching by membrane extrinsic iodide anion (Stubbs et al., 1976), suggests in general an intrinsic and shielded bilayer location for the probe. Definitive determination of probe location can be achieved only by using oriented lipid multilayers; most previous oriented studies (Kooyman et al., 1983; Arcioni and Zannoni, 1984; van der Meer et al., 1984) have focused experimentally on the study of rodlike molecules (e.g., DPH) embedded in liquid crystalline lipid bilayers, in contrast to disc-shaped molecules (e.g., perylene), as discussed here (Chong et al., 1985). These studies suggest a possible subpopulation of molecules oriented parallel to the membrane surface and lying between the acyl chain leaflets (i.e., probe heterogeneity in contrast to lipid heterogeneity). Moreover, transverse mobility of DPH across the bilayer width has been reported, with the actual probe distribution dependent on the physical state of the bilayer (Davenport et al., 1985; Pebay-Peyroula et al., 1994). Alternatively, a fixed localization for the probe can be achieved by anchoring the fluorophore to the phospholipid backbone. Preliminary studies using coronene tagged in this fashion have revealed (Shen et al., 1994) data consistent with our "free" coronene model (data to be presented in detail elsewhere), suggesting that if a probe population does indeed exist between the bilayer leaflets, the overall interpretations presented here still apply.

Experiments using SUVs colabeled with DPH and coronene suggest no probe-induced bilayer perturbations; DSC studies of such bilayer-probe systems can only furnish information on gross macro-bilayer perturbations. Further-

more, as discussed in the Results, no evidence of preferential partitioning for coronene in "gel" and/or "fluid" lipid is suspected. The broadening of the transition profile is due to the long fluorescence lifetime of the probe (Davenport and Targowski, 1995).

Based on experimentally obtained, time-resolved polarized emission data for coronene embedded in single-component lipid bilayers, we have adopted two simple membrane models. Both bilayer models assume heterogeneity of lipid packing and envisage the bilayer composed of coexisting "gel" and "fluid" lipid phases. Previous membrane probe studies using fluorescence associative spectral techniques have eluded to the coexistence of heterogeneous "gel" and "fluid" lipid microenvironments in vesicles composed of a single phosphoglyceride type (Davenport et al., 1986). Similar conclusions were reached by Chong and Weber (1983), using hydrostatic pressure studies of DPH in lipid multilayers, by Parassasi et al. (1993) using laurdan, and by Ruggiero and Hudson (1989) and Mateo et al. (1993a,b) using all *trans*-parinaric acid, where the latter two probes possess spectral and lifetime sensitivity to the gel-fluid microenvironment. Furthermore, Kristovitch and Regen (1991) have isolated lipid dimers through self-recognition, using HPLC methodologies. Alternative homogeneous models (e.g., "wobbling in a cone" or other potentials) have assumed homogeneity of the lipid matrix when analyzing rotational data for fluorescence probes (Kawato et al., 1977; Zannoni, 1981). In reality, it is reasonable to expect that both heterogeneous and homogeneous lipid packing models contribute to a more realistic picture of the bilayer matrix of membranes.

As predicted by the compartmental model, the effective rotational correlation time (ϕ_{EFF}) for coronene embedded in DPPC SUVs ranged from 180 to 15 ns, over the corresponding temperature range (7 to 41°C), resulting in lipid exchange or fluctuation rates of 5.5×10^6 and 6.6×10^7 s^{-1}, respectively. These data compare favorably with other studies. Using all *trans*-parinaric acid, Ruggiero and Hudson (1989) report critical density lipid fluctuation times for DPPC, around 10 ns at 42°C, whereas lipid relaxation times around 30 ns (at 42°C) for DPPC have been measured from ultrasound studies (Mitaku et al., 1983; Michels et al., 1989). These submicrosecond depolarizing motions as reported here are clearly too fast to represent whole vesicle rotation (microsecond time scale; see below) and too slow to represent rotation of coronene in the fluid lipid phase (a few nanoseconds). We propose that such probe rotational motions reflect slow acyl chain fluctutations of the phospholipid matrix and are characteristic of the equilibrium "melt" process between gel and fluid lipid (k_{FG}).

The application of probes with long fluorescence lifetimes (several hundreds of nanoseconds) to studies of lipid dynamics presents some unique problems. Rotational depolarizations arising from whole vesicle rotation (Zannoni, 1981) or, alternatively, from two-dimensional lateral diffusion may cause erroneous interpretations. Estimations of rotational correlation times calculated from the Perrin equation (Chen et al., 1977) for a spherical SUV with an average diameter of 250 Å (determined from electron microscopy studies, described elsewhere; Davenport et al., 1985) are 3.90 μs at 0°C and 2.02 μs at 25°C. Hence, even within the extended time window used here, rotational depolarization of the observed fluorescence arising from simple whole vesicle rotation of immobile probe molecules (N) will not be visible as a separate decay component. However, toward T_c, extracted rotational correlation times for coronene are significantly faster (by a factor of at least 10) than can be accounted for by whole vesicle rotation and can only represent probe embedded in gel regions, i.e., nonexchangeable lipid fraction (N). Similar data were obtained for LUVs; long rotational times (several hundred nanoseconds) (ϕ_N) appear to be independent of vesicle size and more dependent on the physical state of the lipids. Moreover, values for lateral diffusion coefficients for lipids within synthetic bilayers are reported (Jacobson, 1983) to fall within the range 10^{-10} cm^2/s (below T_c) to 10^{-8} cm^2/s (above T_c). By relating lateral rotational correlation times (ϕ_D) with reported lateral diffusion coefficients (Quitevis et al., 1993), estimated values for ϕ_D are around 4 ms (below T_c) for DPPC SUVs. Thus for studies described here, which focus on lipid fluctuations occurring below T_c, recovered rotational parameters do not appear to be contaminated by lateral diffusion effects of coronene (with increasing temperature).

Analysis of time-resolved polarized data using our Landau-derived "gated" fluctuation model provides several attractive features over the more simplistic compartmental model. Experimental values for a lipid gating factor (γ) or required multiple of the E_{ACT} barrier may be determined. This essentially provides an estimate of the number of lipid molecules (or cluster size) surrounding the fluorescence probe that must undergo acyl-chain fluidization, enabling rotational freedom of embedded coronene. Unlike cluster sizes determined from DSC studies (Biltonen, 1990), here the value of γ represents an E_{ACT} penalty for fluidization of those neighboring lipids that directly affect rotational motions of coronene. From the overall headgroup surface area for DPPC of 50 ± 2 $Å^2$ (below the phase transition; Janiak et al., 1976) and the dimensions of the coronene carbon skeleton (diameter approximately 7.4 Å), recovered values of the gating factor suggest that several lipid shells surround the probe and are involved in the lipid chain disordering process, with estimated "cluster" sizes on the order of 25–40 Å in diameter. Recently, Parassasi et al. (1993) estimated cluster sizes ranging from 20 to 50 Å using preferential partitioning of laurdan embedded in a two-component lipid system. As expected, cluster sizes determined by local or short-range spectroscopic methods are significantly smaller than those determined by long-range DSC methods.

Insights into the local bilayer microenvironment surrounding coronene may be ascertained from the limiting rotational rate parameter (d_∞). The concept of lipid bilayer microviscosity has been the focus of numerous fluorescence probe investigations (Shinitzky, 1984). It is now well estab-

lished that because of the anisotropic nature of the membrane, determination of the so-called membrane "microviscosity" via the Perrin equation, by comparison of rotational motions of a dye in an isotropic solvent system of appropriate macroviscosity, is not valid. Because rotational motions of short-lived fluorescence membrane probes occurring on the nanosecond time scale (as discussed above) very often reveal a limiting anisotropy term (r_∞), submicrosecond lipid dynamics are obscured from detection ($\tau_{FL} < \phi$) and a complete dynamic picture of the bilayer is not possible on this time scale. Because the use of long-lived fluorescence probes provides a broader averaging range over which the dynamic heterogeneity can be viewed ($\tau_{FL} > \phi$), values for d_∞ have the potential to more closely reflect the immediate "local" environment surrounding the probe. In contrast to other membrane ordering studies, our "gated" fluctuation model is probe independent; inherent in its derivation are the thermodynamic properties of the matrix lipid (in this case DPPC). As such we may expect that time-resolved emission anisotropy profiles obtained for a wide range of fluorescence probes (with varying lifetimes) embedded in lipid bilayer systems and selectively sensitive to lipid fluctuations (as discussed above) may be successfully described by this model.

Simple Landau modeling requiring only three fitting parameters has led to a distribution of lipid order-induced submicrosecond exchange rates ($d(S,T)$) at each temperature, with considerable correspondence to our experimental observations. Because other currently available lipid membrane models are unable to predict submicrosecond lipid melting rates, our model provides an alternative view of bilayer lipid dynamics. However, limitations of our mean-field model apply, and more appropriate descriptions involving refined compartmental-like models may ultimately be more appropriate. In particular, Landau theory describes long-range pretransitional fluctuations occurring during the second-order lipid phase transitions and inherently assumes equal partitioning of probes into all regions of the bilayer. Although the lipid "melt" transition has been classed as weakly first order (Mitaku et al., 1983), the Landau fluctuation theory has been applied successfully to the intepretation of other lipid dynamic data (Jähnig, 1981a,b; Mitaku et al., 1983; Goldstein and Leibler, 1989). Consistent with our microheterogeneous lipid packing model of the bilayer, lipid fluctuations are local and occur over a short range. However, by undergoing conformational lipid fluctuations, a more ordered long-range positional disordering effect occurs, resulting ultimately in lipid cluster fluidization. We believe our application here remains valid; development of Landau theory from first principles involves a microsystem that fluctuates from equilibrium (Landau and Lifchitz, 1958).

In summary, we have attempted here to explore submicrosecond lipid dynamics using a new fluorescence probe coronene, which combined with its long fluorescence lifetime and selective out-of-plane rotational motions, provides an attractive probe for such studies. Rotational motions for this probe may be interpretated using two alternative lipid models, both invoking an exchange process between "gel" and "fluid" regions of a heterogeneously packed bilayer. We are currently (Shen et al., 1994) exploring the effects of biological modulators (e.g., anesthetics, cholesterol, peptides, and proteins) on lipid fluctuation rates. Such investigations may ultimately have clinical significance for membrane-associated disorders.

We thank Bo Shen for assistance with sample preparations and Salvatore Atzeni for help in acquiring time-resolved fluorescence data. We express gratitude to Dr. Jay R. Knutson, Professor Ludwig Brand, and Professor Tadeusz Marszalek for helpful and insightful discussions. We are grateful to Hazel Ward for assistance with manuscript preparation and Michael P. Straher for graphic arts presentation.

This research was supported in part by the American Heart Association, New York City Affiliate; the National Science Foundation, Award no. DMB-9006044; the PSC-CUNY Internal Award Program; and the Petroleum Research Fund of the American Chemical Society. LD was an Investigator of the American Heart Association, New York City Affiliate.

REFERENCES

Albrecht, O., H. Gruler, and E. Sackmann. 1978. Polymorphism of phospholipid monolayers. *J. Physiol. (Paris).* 39:301–313.

Arcioni, A., and C. Zannoni. 1984. Intensity deconvolution in fluorescence depolarization studies of liquids, liquid crystals and membranes. *Chem. Phys.* 88:113–128.

Badea, M. G., and L. Brand. 1979. Time resolved fluorescence measurements. *Methods Enzymol.* 61:378–394.

Barenholz, Y., D. Gibbes, B. J. Litman, J. Goll, T. E. Thompson, and F. D. Carlson. 1977. A simple method for the preparation of homogeneous phospholipid vesicles. *Biochemistry.* 16:2806–2810.

Barkley, M. D., A. A. Kowalczyk, and L. Brand. 1981. Fluorescence decay studies of anisotropic rotations of small molecules. *J. Chem. Phys.* 75:3581–3593.

Beechem, J. M., and L. Brand. 1986. Global analysis of fluorescence decay: applications to some unusual experimental and theoretical studies. *Photochem. Photobiol.* 44:323–329.

Beechem, J. M., J. R. Knutson, and L. Brand. 1984. Global analysis of fluorescence emission and anisotropy decay: associative and non-associative modeling. *Photochem. Photobiol.* 39:41S.

Biltonen, R. 1990. A statistical-thermodynamic view of cooperative structural changes in phospholipid bilayer membranes: their potential role in biological function. *J. Chem. Thermodyn.* 22:1–19.

Brand, L., J. R. Knutson, L. Davenport, J. M. Beechem, R. E. Dale, D. G. Walbridge, and A. A. Kowalczyk. 1985. Time-resolved fluorescence spectroscopy: some applications of associative behaviour to studies of proteins and membranes. *In* Spectroscopy and the Dynamics of Molecular Biological Systems. P. M. Bayley and R. E. Dale, editors. Academic Press, London. 259–305.

Brandt, S. 1970. Statistical and Computational Methods in Data Analysis. North Holland Publishing Company, Amsterdam and London.

Brown, M. F., and J. Seelig. 1979. Structural dynamics in phospholipid bilayers from deuterium spin-lattice relaxation time measurements. *J. Chem. Phys.* 70:5045–5053.

Brunner, J., P. Skrabal, and H. Hauser. 1976. Single bilayer vesicles prepared without sonication. Physico-chemical properties. *Biochim. Biophys. Acta.* 455:322–331.

Chapman, D., R. M. Williams, and B. D. Ladbrooke. 1967. Physical studies of phospholipids. VI. Thermotrophic and lyotrophic mesomorphism of some 1,2-diacyl-phosphatidylcholines (lecithins). *Chem. Phys. Lipids.* 1:445–475.

Chen, L. A., R. E. Dale, S. Roth, and L. Brand. 1977. Rotational relaxation of the "microviscosity" probe diphenylhexatriene in paraffin oil and egg lecithin vesicles. *J. Biol. Chem.* 252:7500–7510.

Chen, R. F., and R. L. Bowman. 1963. Fluorescence polarization: measurement with ultraviolet-polarizing filters in a spectrophotofluorometer. *Science.* 147:729–732.

Chong, L-G., B. W. van der Meer, and T. E. Thompson. 1985. The effects of pressure and cholesterol on rotational motions of perylene in lipid bilayers. *Biochim. Biophys. Acta.* 813:253–265.

Chong, L. G., and G. Weber. 1983. Pressure dependence of 1,6-diphenyl-1,3,5-hexatriene fluorescence in single-component phosphatidylcholine liposomes. *Biochemistry.* 22:5544–5550.

Davenport, L., R. E. Dale, R. H. Bisby, and R. B. Cundall. 1985. Transverse location of the fluorescent probe 1,6-diphenyl-1,3,5-hexatriene in model lipid bilayer membrane systems by resonance excitation energy transfer. *Biochemistry.* 24:4097–4108.

Davenport, L., J. R. Knutson, and L. Brand. 1986. Anisotropy decay associated fluorescence spectra and analysis of rotational heterogeneity. 2. 1,6-diphenyl-1,3,5-hexatriene in lipid bilayers. *Biochemistry.* 25: 1811–1816.

Davenport, L., J. R. Knutson, and L. Brand. 1988. Time-resolved fluorescence anisotropy of membrane probes: rotations gated by packing fluctuations. *Proc. Int. Soc. Opt. Eng.* 909:263–270.

Davenport, L., J. R. Knutson, and L. Brand. 1989. Fluorescence studies of membrane dynamics and heterogeneity. *Subcell. Biochem.* 14:145–188.

Davenport, L., and P. Targowski. 1993. Effects of pressure on submicrosecond lipid dynamics using a long-lived fluorescence probe. *Biophys. J.* 64:A75.

Davenport, L., and P. Targowski. 1995. Long-lived probes for studying lipid dynamics: a review. *J. Fluoresc.* 5:9–18.

Davenport, L., P. Targowski, and J. R. Knutson. 1995. Volume fluctuations in lipid bilayers. High pressure time-resolved fluorescence studies. *Biophys. J.* 68:A303.

deGennes, P. G., and J. Prost. 1993. The Physics of Liquid Crystals. Oxford University Press, New York.

Dittmer, J. C., and R. L. Lester. 1964. A simple, specific spray for the detection of phospholipids on thin-layer chromatograms. *J. Lipid Res.* 5:126–127.

Doniach, S. 1978. Thermodynamic fluctuations in phospholipid bilayers. *J. Chem. Phys.* 68:4912–4916.

Edidin, M. 1992. Patches, posts and fences: proteins and plasma membrane domains. *Trends Cell Biol.* 2:376–380.

Goldstein, R. E., and S. Leibler. 1989. Structural phase transitions of intercating membranes. *Phys. Rev. A.* 40:1025–1035.

Hauser, H. O. 1971. The effect of ultrasonic irradiation on the chemical structure of egg lecithin. *Biochem. Biophys. Res. Commun.* 45: 1049–1055.

Hawton, M. H., and J. W. Doane. 1987. Pretransitional phenomena in phospholipid/water multilayers. *Biophys. J.* 52:401–404.

Heyn, M. P. 1979. Determination of lipid order parameters and rotational correlation times from fluorescence depolarization experiments. *FEBS Lett.* 108:359–364.

Hope, M. J., M. B. Bally, G. Webb, and P. R. Cullis. 1985. Production of large unilamellar vesicles by a rapid extrusion procedure. Characterization of size distribution, trapped volume and ability to maintain a membrane potential. *Biochim. Biophys. Acta.* 812:55–65.

Hubbell, W. L., and H. M. McConnell. 1971. Molecular motion in spin-labeled phospholipids and membranes. *J. Am. Chem. Soc.* 93:314–326.

Husain, M., D. E. Edmondson, and T. P. Singer. 1982. Kinetic studies on the catalytic mechanism of liver monoamine oxidase. *Biochemistry.* 21:595–600.

Imaizumi, S., and C. W. Garland. 1987. A.c. calorimetric studies of main transition in dipalmitoylphosphatidylcholine. *J. Phys. Soc. Jpn.* 56: 3887–3892.

Ipsen, J. H., K. Jorgensen, and O. G. Mouritsen. 1990. Density fluctuations in saturated phospholipid bilayers increase as the acyl chain length decreases. *Biophys. J.* 58:1099–1107.

Jablonski, A. 1950. Fundamental polarization of photoluminescence and torsional vibrations of molecules. *Acta Physiol. Pol.* 10:193–206.

Jacobson, K. 1983. Lateral diffusion in membranes. *Cell Motil.* 3:367–373.

Jähnig, F. 1979. Structural order of lipids and proteins in membranes: evaluation of fluorescence anisotropy data. *Proc. Natl. Acad. Sci. USA.* 76:6361–6365.

Jähnig, F. 1981a. Critical effects from lipid-protein interactions in membranes. I. Theoretical descriptions. *Biophys. J.* 36:329–345.

Jähnig, F. 1981b. Critical effects from lipid-protein interactions in membranes. II. Interpretation of experimental results. *Biophys. J.* 36: 347–357.

Janiak, M. J., D. M. Small, and G. G. Shipley. 1976. Nature of the thermal pretransition of synthetic phospholipids: dimyristoyl- and dipalmitoyllecithin. *Biochemistry.* 15:4575–4580.

Jost, P., A. S. Waggoner, and O. H. Griffith. 1971. Spin labeling and membrane structure. *In* Structure and Function of Biological Membranes. L. I. Rothfield, editor. Academic Press, New York. 83–144.

Kanehisa, M. I., and T. Y. Tsong. 1978. Cluster model of lipid phase transitions with application to passive permeation of molecules and structure relaxations in lipid bilayers. *J. Am. Chem. Soc.* 100:424–432.

Katraro, R., A. Ron, and S. Speiser. 1979. Photophysical studies of coronene and 1,12-benzperylene, self-quenching, photoquenching, temperature dependent fluorescence decay and temperature dependent electronic energy transfer to dye acceptors. *Chem. Phys.* 42:121–132.

Kawato, S., K. Kinosita, and A. Ikegami. 1977. Dynamic studies of lipid bilayers studied by nanosecond fluorescence techniques. *Biochemistry.* 16:2319–2324.

Klausner, R. D., A. M. Kleinfeld, R. L. Hoover, and M. J. Karnovsky. 1980. Lipid domains in membranes. Evidence derived from structural perturbations induce by free fatty acids and lifetime heterogeneity analysis. *J. Biol. Chem.* 255:1286–1295.

Knutson, J. R., J. M. Beechem, and L. Brand. 1983. Simultaneous analysis of multiple fluorescence decay curves: a global approach. *Chem. Phys. Lett.* 102:501–507.

Kooyman, R. P. H., M. H. Vos, and Y. K. Levine. 1983. Determination of orientational order parameters in oriented lipid membrane systems by angle-resolved fluorescence depolarization experiments. *Chem. Phys.* 81:461–472.

Kristovitch, S. M., and S. L. Regen. 1991. Nearest neighbor recognition in phospholipid bilayers. Probing lateral organization at the molecular level. *J. Am. Chem. Soc.* 113:8175–8180.

Lakowicz, J. R., and J. R. Knutson. 1980. Hindered depolarizing rotations of perylene in lipid bilayers. Detection by lifetime-resolved fluorescence anisotropy measurements. *Biochemistry.* 19:905–911.

Lakowicz, J. R., F. G. Prendergast, and D. Hogan. 1979. Differential polarized fluorescence investigations of diphenylhexatriene in lipid bilayers. Quantitation of hindered depolarizing rotations. *Biochemistry.* 18:508–519.

Lamotte, M., and J. Joussot-Dubien. 1974. Dispersion states and orientation of aromatic solutes in monocrystalline matrices of *n*-heptane. *J. Chem. Phys.* 61:1892–1898.

Lamotte, M., A. M. Merle, J. Joussot-Dubien, and F. Dupuy. 1975. Multiplet structure of the emission bands of coronene and perylene in *n*-heptane single crystal. *Chem. Phys. Lett.* 35:410–416.

Landau, L. D., and E. M. Lifchitz. 1958. Statistical Physics. Pergamon Press, London.

Lee, A. G. 1977. Lipid phase transitions and phase diagrams. I. Lipid phase transitions. *Biochim. Biophys. Acta.* 472:237–281.

Lentz, B. R., Y. Barenholz, and T. E. Thompson. 1976. Fluorescence depolarization studies of phase transition and fluidity in phospholipid bilayers. 2. Two-component phosphatidylcholine liposomes. *Biochemistry.* 15:4529–4537.

Lewis, C., W. R. Ware, L. J. Doemeny, and T. L. Nemzek. 1973. Meaurement of short-lived fluorescence decay using the single photon counting method. *Rev. Sci. Instrum.* 44:107–114.

Lunde, K., and L. Zechmeister. 1954. *cis-trans* isomeric 1,6-diphenylhexatrienes. *J. Am. Chem. Soc.* 76:2308–2313.

Mateo, C. R., J. C. Brochon, M. P. Lillo, and U. A. Acuna. 1993a. Lipid clustering in bilayers detected by the fluorescence kinetics and anisotropy of *trans*-parinaric acid. *Biophys. J.* 65:2237–2247.

Mateo, C. R., M. P. Lillo, J. Gonzalez-Rodriguez, and A. U. Acuna. 1991. Lateral heterogeneity in human platelet plasma membranes and lipids from time-resolved fluorescence of *trans*-parinaric acid. *Eur. Biophys. J.* 20:53–59.

Mateo, C. R., P. Tauc, and J. C. Brochon. 1993b. Pressure effects on the physical propertes of lipid bilayers detected by *trans*-parinaric acid fluorescence decay. *Biophys. J.* 65:2248–2260.

McClare, C. W. F. 1971. An accurate and convenient organic phosphorus assay. *Anal. Biochem.* 39:527–530.

Melchior, D. L., and J. M. Steim. 1976. Thermotropic transitions in biomembranes. *Annu. Rev. Biophys. Bioeng.* 5:205–238.

Mendelson, R., S. Sunder, and H. J. Bernstein. 1976. The effect of sonication on the hydrocarbon chain conformation in model membrane systems: a Raman spectroscopic study. *Biochim. Biophys. Acta.* 419: 563–569.

Michels, B., N. Fazel, and R. Cerf. 1989. Enhanced fluctuations in small phospholipid bilayer vesicles containing cholesterol. *Eur. Biophys. J.* 17:187–190.

Michl, J., and E. W. Thulstrup. 1986. Spectroscopy of Polarized Light. VCH Publishers, New York. 488–539.

Mitaku, S., A. Ikegami, and A. Sakanishi. 1978. Ultrasonic stiudies of lipid bilayers. Phase transition in synthetic phosphatidylcholine liposomes. *Biophys. Chem.* 8:295–304.

Mitaku, S., T. Jippo, and R. Kataoka. 1983. Thermodynamic properties of the lipid bilayer transition. Pseudocritical phenomena. *Biophys. J.* 42: 137–144.

Mouritsen, O. G., A. Boothroyd, R. Harris, N. Jan, T. Lookman, L. MacDonald, D. A. Pink, and M. J. Zuckerman. 1983. Computer simulation of the main gel-fluid phase transition of lipid bilayers. *J. Chem. Phys.* 79:2027–2041.

Mouritsen, O. G., and M. J. Zuckerman. 1985. Softening of lipid bilayers. *Eur. Biophys. J.* 12:75–86.

Nagle, J. F., and J. L. Scott, Jr. 1978. Lateral compressibilty of mono- and bilayers. Theory of membrane permeability. *Biochim. Biophys. Acta.* 513:236–243.

Parker, C. A., and W. T. Rees. 1962. Fluorescence spectrometry—a review. *Analyst (Lond.).* 87:83–111.

Parassasi, T., A. M. Giusti, E. Gratton, E. Monaco, M. Raimondi, G. Ravagnan, and O. Sapora. 1994. Evidence for an increase in water concentration in bilayers after oxidative damage of phospholipids induced by ionizing radiation. *Int. J. Radiat. Biol.* 65:329–334.

Parassasi, T., G. Ravagnan, R. M. Rusch, and E. Gratton. 1993. Modulation and dynamics of phase properties in phospholipid mixtures detected by Laurdan fluorescence. *Photochem. Photobiol.* 57:403–410.

Pebay-Peyroula, E., E. J. Dufourq, and A. G. Szabo. 1994. Location of diphenyl-hexatriene and triethylammonium-diphenyl-hexatriene in dipalmitoylphosphatidylcholine bilayers by neutron diffraction. *Biophys. Chem.* 53:45–56.

Quitevis, E. L., A. H. Marcus, and M. D. Fayer. 1993. Dynamics of ionic lipophilic probes in micelles: picosecond fluorescnce depolarization measurements. *J. Phys. Chem.* 97:5762–5769.

Ruggiero, A., and B. S. Hudson. 1989. Critical density fluctuations in lipid bilayers detected by fluorescence lifetime heterogeneity. *Biophys. J.* 55:1111–1124.

Sassaroli, M., M. Vauhkonen, P. Somerharju, and S. Scarlatta. 1993. Dipyrenyl phosphatidylcholines as membrane fluidity probes. Pressure and temperature dependence of the intramolecular excimer formation rate. *Biophys. J.* 64:137–149.

Seelig, A., and J. Seelig. 1974a. The dynamic structure of fatty acyl chains in a phospholipid bilayer measured by deuterium magnetic resonance. *Biochemistry.* 13:4839–4845.

Seelig, J., and A. Seelig. 1974b. Deuterium magnetic resonance studies of phospholipid bilayers. *Biochem. Biophys. Res. Commun.* 57:406–410.

Seiter, C. H. A., and S. I. Chan. 1973. Molecular motion in lipid bilayers. A nuclear magnetic resonance line width study. *J. Am. Chem. Soc.* 95:7541–7553.

Shen, B., P. Targowski, J. Lobo, and L. Davenport. 1994. Effects of peptides on submicrosecond lipid dynamics using long-lived fluorescence probes. *Biophys J.* 66:A58.

Shinitzky, M. 1984. Membrane fluidity and cellular functions. *In* Physiology of Membrane Fluidity, Vol. 1. M. Shinitzky, editor. CRC Press, Boca Raton, FL. 1–51.

Sieber, F. 1987. Yearly review. Merocyanine 540. *Photochem. Photobiol.* 46:1035–1042.

Stockton, G. W., C. F. Polnaszek, A. P. Tulloch, F. Hasa, and I. C. P. Smith. 1976. Molecular motion and order in single-bilayer vesicles and multilamellar dispersions of egg lecithin and lecithin-cholesterol mixtures. A deuterium nuclear magnetic resonance study of specifically labeled lipids. *Biochemistry.* 15:954–966.

Stubbs, C. D., C. Ho, and S. J. Slater. 1995. Fluorescence techniques for probing water penetration into lipid bilayers. *J. Fluoresc.* 5:19–28.

Stubbs, G. W., B. J. Litman, and Y. Barenholz. 1976. Microviscosity of the hydrocarbon region of the bovine retinal rod outer segment disk membrane determined by fluorescent probe measurements. *Biochemistry.* 15:2766–2772.

Tan, A. K., and R. Ramsey. 1993. Substrate-specific enhancement of the oxidative half-reaction of monoamine oxidase. *Biochemistry.* 32: 2137–2143.

Targowski, P., X-Q. Gao, and L. Davenport. 1992. Time-resolved anisotropies of long-lived fluorescence probes for studying submicrosecond phospholipid structural fluctuations. *Biophys. J.* 61:A503.

Thomas, J. L., D. Holowka, B. Baird, and W. W. Webb. 1994. Large-scale co-aggregation of fluorescent-lipid probes with cell surface proteins. *J. Cell Biol.* 125:795–802.

Thurlborn, K. R. 1981. The use of N-[9-anthroyloxy] fatty acids as fluorescence probes for biomembranes. *In* Fluorescent Probes. G. S. Beddard and M. A. West, editors. Academic Press, London. 113–141.

van der Heide, U. A., G. van Ginkel, and Y. K. Levine. 1996. DPH is localised in two distinct populations in lipid vesicles. *Chem. Phys. Lett.* 253:118–122.

van der Meer, W., H. Pottel, W. Herreman, M. Ameloot, H. Hendrickx, and H. Schroeder. 1984. Effect of orientational order on the decay of the fluorescence anisotropy in membrane suspensions. A new approximate solution of the rotational diffusion equation. *Biophys. J.* 46:515–523.

Vercer, J., A. Kowalczyk, and R. E. Dale. 1993. Improved recursive convolution integral for the analysis of fluorescence decay data: local approximation of the apparatus response function by a general polynomial. Rev. Sci. Inst. 64:3403–3412.

Vincent, M., B. deForesta, J. Gallay, and A. Alfsen. 1982. Nanosecond fluorescence anisotropy decays of *N*-(9-anthroyloxy) fatty acids in dipalmitoylphosphatidylcholine vesicles with regard to isotropic solvents. *Biochemistry.* 21:708–716.

Wahl, Ph., J. C. Auchet, and B. Donzel. 1974. The wavelength dependence of the response of a pulse fluorometer using the single photoelectron counting method. *Rev. Sci. Instrum.* 45:28–32.

Wang, S., J. M. Beechem, E. Gratton, and M. Glaser. 1991. Orientational distribution of 1,6-diphenyl-1,3,5-hexatriene in phospholipid vesicles as determined by global analysis of fequency domain fluorimetry data. *Biochemistry.* 30:5565–5572.

Wardlaw, J. R., W. H. Sawyer, and K. Ghiggino. 1987. Vertical fluctuations of phospholipid acyl chains in bilayers. *FEBS Lett.* 223:20–24.

Wolber, P. K., and B. S. Hudson. 1981. Fluorescence lifetime and time-resolved polarization anisotropy studies of acyl chain order and dynamics in lipid bilayers. *Biochemistry.* 20:2800–2808.

Wolf, D. E., and J. K. Voglmayr. 1984. Diffusion and regionalization in membranes of maturing ram spermatozoa. *J. Cell Biol.* 98:1678–1684.

Zannoni, C. 1981. A theory of fluorescence depolarization in membranes. *Mol. Phys.* 42:1303–1320.

Zimmerman, H., and N. Joop. 1961. Polarization der elektonenbanden von aromaten. 5. Mitteilung: benzol, coronen, triphenylen, pyren, perylen. *Z. Elektrochem.* 65:138–142.

Zuckermann, M. J., D. A. Pink, M. Costas, and B. C. A. Sanctuary. 1982. A theoretical model for phase transition in lipid monolayers. *J. Chem. Phys.* 76:4206–4216.